

# Periodical rocking long period gratings in PANDA fibers for high temperature and refractive index sensing\*

JIN Wa (金娃)\*\*, BI Wei-hong (毕卫红), FU Xing-hu (付兴虎), and FU Guang-wei (付广伟)

Key Laboratory for Special Fiber and Fiber Sensor of Hebei Province, School of Information Science and Engineering, Yanshan University, Qinhuangdao 066004, China

(Received 1 April 2017; Revised 2 June 2017)

©Tianjin University of Technology and Springer-Verlag GmbH Germany 2017

We report periodical rocking long period gratings (PR-LPGs) in PANDA fibers fabricated with CO<sub>2</sub> laser. The PR-LPGs achieve very high coupling efficiency of 19 dB with 12 periods and a 3.5° twist angle in just one scanning cycle, which is much more effective than the conventional CO<sub>2</sub> laser fabrication technique. This type of LPGs exhibits polarization-selective resonance dips which demonstrate different sensitivities to environmental parameters. The high temperature and external refractive index sensitivities are measured simultaneously, so it can be used as a wavelength-selective polarization filter and sensor.

**Document code:** A **Article ID:** 1673-1905(2017)05-0354-4

**DOI** <https://doi.org/10.1007/s11801-017-7075-9>

A long-period grating (LPG) provides an efficient method to couple light from the guided mode to the cladding modes at specific resonance wavelengths<sup>[1]</sup>, so it has widespread applications in telecommunication<sup>[1]</sup> and sensing<sup>[2]</sup>. Various techniques, such as the traditional UV writing technique<sup>[3]</sup>, femtosecond laser writing technique<sup>[4]</sup>, CO<sub>2</sub> laser irradiation<sup>[5]</sup>, arc discharge<sup>[6]</sup>, and chemical etching technique<sup>[7]</sup>, are used to fabricate LPGs in the standard telecommunication fibers. Apart from single-mode fibers, LPGs have been fabricated in polarization-maintaining (PM) fibers for applications as in-fiber polarizers and sensors<sup>[8,9]</sup>. Because of the birefringence in a PM fiber, the coupling to the same order cladding mode generates two resonance wavelengths corresponding to two orthogonal polarization states of the fiber.

Recently, an LPG with a helix-profile refractive index modulation has been reported<sup>[10-12]</sup>. This helical index modulation was induced by CO<sub>2</sub> laser irradiation on one side of the fiber, while the fiber was continuously rotated around and translated longitudinally along its axis.

In this paper, we report a novel type of LPGs by rocking a PM fiber back and forth to induce permanent twists periodically along the fiber. As known, periodical rotation forth and back around the principle axis of PM fiber can induce polarization rocking filters (PRFs)<sup>[13]</sup> which couple the two polarization states of fundamental mode when a pitch is the beat length, as shown in Fig.1(a) and (b). However, when the pitch satisfies the phase-match condition of coupling between core mode and cladding mode while the twist is induced by asymmetric CO<sub>2</sub> laser irradiation, which results in the permanent torsion strain in the

cross-section of the fiber and the refractive index periodical modulation<sup>[14]</sup>, as shown in Fig.1(c) and (d), the PR-LPG appears.

The mode coupling for the PR-LPG may be complex. In the CO<sub>2</sub> laser irradiation region, the twist induces torsion strain, which results in changes in the refractive index or the dielectric permittivity. Since the CO<sub>2</sub> laser is irradiated from one side of the fiber, asymmetric change of permittivity will occur in the cross-section of the CO<sub>2</sub> laser irradiated section. The periodic perturbation of the permittivity along the fiber, according to the well-known coupled-mode theory, results in resonant coupling between the fundamental core mode and higher order cladding modes and forms an LPG.

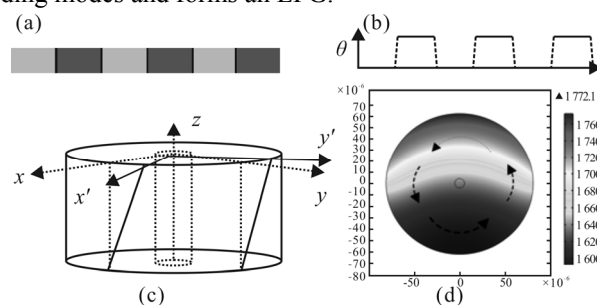


**Fig.1 (a) Schematic of PR-LPG (The dark grey sections have a rotation angle of  $\theta$  with respect of the light grey sections. The black section is twist.); (b) Angle profile along fiber; (c) Twisted fiber; (d) Temperature distribution of the cross-section of the fiber**

In the CO<sub>2</sub> laser irradiated region, the twist induces torsion strain, which results in changes in the refractive

\* This work has been supported by the National Natural Science Foundation of China (No.61605168), the Natural Science Foundation of Hebei Province (No.F2016203392), the College and University Natural Science Foundation of Hebei Province (No.QN2016078), the Science and Technology Project of Qinhuangdao City (No.201601B050), and the Intramural Doctoral Foundation of Yanshan University (No.B1011).

\*\* E-mail: jinwa@ysu.edu.cn

index or the dielectric permittivity<sup>[15]</sup>. The perturbation of the dielectric tensor may be written in the form of

$$\boldsymbol{\varepsilon}(z) = R(\theta) \begin{pmatrix} \varepsilon_a & 0 \\ 0 & \varepsilon_b \end{pmatrix} R(-\theta) f(z) \quad (1)$$

where  $\varepsilon_a$  and  $\varepsilon_b$  are respectively the effective refractive indices of the fast mode and slow mode in the CO<sub>2</sub> laser irradiated region. They are affected by the built-in shear stress, which are mainly determined by the magnitude of the applied twist.  $\theta$  is an effective twist angle.  $R(\theta)$  is

$$R(\theta) = \begin{pmatrix} \cos \theta & -\sin \theta \\ \sin \theta & \cos \theta \end{pmatrix} \quad (2)$$

$f(z)$  is a periodic function of  $z$  and takes non-zero value only in the CO<sub>2</sub> laser irradiated region.  $f(z)$  may be expressed in terms of a Fourier series as

$$f(z) = \sum_{m=0} f_m \exp \left[ -im \left( \frac{2\pi}{\Lambda} \right) z \right] \quad (3)$$

The induced change in the dielectric tensor may then be expressed as

$$\Delta \boldsymbol{\varepsilon} = \sum_{m=0} \boldsymbol{\varepsilon}_m \begin{pmatrix} -\sin^2 \theta & -\sin \theta \cos \theta \\ \sin \theta \cos \theta & \sin^2 \theta \end{pmatrix} \times \exp \left[ -im \left( \frac{2\pi}{\Lambda} \right) z \right] \quad (4)$$

where  $\boldsymbol{\varepsilon}_m$  is related to  $\varepsilon_a$ ,  $\varepsilon_b$  and  $f_m$  which are difficult to be quantified since the exact distribution of permittivity variation is not known.

The coupled-mode equation for the fundamental core mode may be derived as

$$\begin{pmatrix} \frac{\partial A_{co}^H}{\partial z} \\ \frac{\partial A_{co}^V}{\partial z} \end{pmatrix} = -iC_m \text{sign}(\beta_{co}) \times \begin{pmatrix} \sin^2 \theta \langle E_{co}^H | E_{cl}^H \rangle & -\sin \theta \cos \theta \langle E_{co}^H | E_{cl}^V \rangle \\ \sin \theta \cos \theta \langle E_{co}^V | E_{cl}^H \rangle & -\sin^2 \theta \langle E_{co}^V | E_{cl}^V \rangle \end{pmatrix} \times \begin{pmatrix} A_{cl}^H \\ A_{cl}^V \end{pmatrix} \exp \left[ i \left( \beta_{co} - \beta_{cl} - m \frac{2\pi}{\Lambda} \right) z \right] \quad (5)$$

where  $A_i^H$  and  $A_i^V$  are the field amplitudes for the horizontal and vertical polarization states, respectively.  $\langle E_{co}^H | E_{co}^H \rangle = \iint E_{co}^{H*} E_{cl}^H dx dy$  is the field overlap integral of the core and cladding modes, and  $C_m$  is a coupling coefficient for the  $m$ th order grating. When the twist angle  $\theta$  is small, the term of  $\sin^2 \theta$  may be neglected, then the coupling constant can be expressed as

$$\kappa_m = \frac{C_m}{2} \sin 2\theta \iint E_{co}^{V*} E_{cl}^H dx dy = \frac{C_m}{2} \sin 2\theta \iint E_{co}^{H*} E_{cl}^V dx dy \quad (6)$$

The experimental setup is shown in Fig.2(a). A polarizer is used to launch linearly polarized light to a section of PANDA fiber (birefringence of  $5 \times 10^{-4}$ ). The PMF is fixed to two clamps with 12 cm separation between them.

One clamp is fixed to a motor-driving rotation stage that could oscillate at a fixed angle with a constant speed at a given frequency controlled by Labview program, shown in Fig.2(b), which can control the fiber to rotate back and forth automatically. During scanning, the high-frequency CO<sub>2</sub> laser pulses hit the fast axis of the PMF repeatedly and induce a local high temperature to soften the silica of the fiber. By applying a small twist, a small permanent rotation is induced in the soften region. The schematic structure of the twisted PANDA fiber is shown in Fig.3.

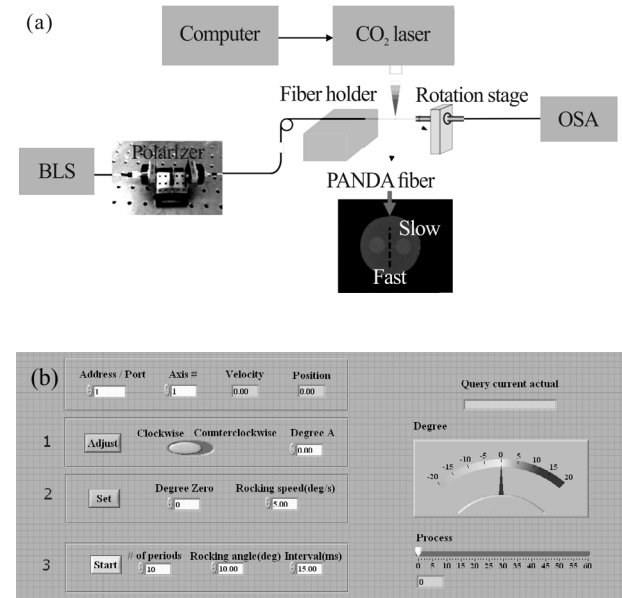


Fig.2 (a) Experimental setup for fabrication of PR-LPGs in PANDA fiber; (b) Operation interface of the fabrication system

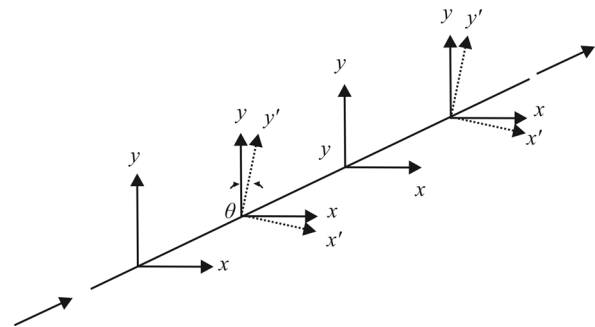
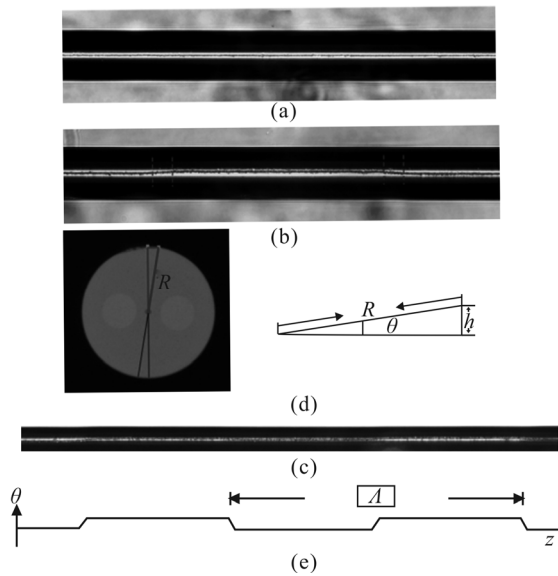


Fig.3 Schematic diagram of the structure of PR-LPG in PMFs

In order to distinguish the twist angle, before fabricating the gratings, a straight line was carved on the surface of the PANDA fiber by a femtosecond infrared laser, as shown in Fig.4(a), serving as a marker to visualize the induced twist along the optical fiber. Fig.4(b) shows a particular twist profile when rotating the clamp by 15°. A rocking angle profile as a function of position along the fiber is given in Fig.4(b): the twist region is about 50  $\mu\text{m}$  long and the separation between the two twists is 475  $\mu\text{m}$ ,

which means the pitch of this grating is about 950 μm. The actual twist angle is directly measured from the microscope image of Fig.4(b), from which  $h$  in Fig.4(c) can be read directly,  $R$  is the radius of fiber, and  $\theta$  can be calculated by  $\theta = \arcsin(h/R)$  and found to be about 3.5°, indicating about 1/3 of the applied rotation is transferred to permanent twists in CO<sub>2</sub> laser heated regions. Fig.4(d) and (e) show the twist angle profile along the fiber.



**Fig.4 A PR-LPG fabricated in a PANDA fiber: (a) Microscope image before rotating; (b) The angle profile along the fiber; (c) Schematic diagram of calculating rocking angle; (d) and (e) Rocking angle profile along the fiber**

Fig.5 shows the normalized transmission spectra of the PR-LPG in a PANDA fiber. The resonance wavelengths for the two polarization modes are 1 537.2 nm and 1 546.2 nm, respectively, and the corresponding grating intensities are 19.2 dB and 15.2 dB, respectively. The insertion loss of the PR-LPG is ~ 0.7 dB.

By using mode index and field distribution of the PANDA fiber and  $C_m$  as variable fitting parameters, we calculate the transmission of coupling between the fast mode and the cladding mode for a PR-LPG, as shown in Fig.5. The calculated transmission spectra agree well with the experimental results demonstrated in Fig.6.

From Eq.(6), it is seen that the twist angle will affect the coupling constant through  $\sin 2\theta$  as well as  $C_m$ , which is also affected by  $\theta$  through the shear stress-induced perturbation of the permittivity. The larger the twist angle, the bigger the induced torsion strain, and the more the change in permittivity. The pitches which make the full coupling condition satisfied depend on the twist angle, as shown in Fig.7, which provides an effective technique to adjust the device length and the bandwidth of the filters.

One of the potential applications of the novel LPGs is for sensing. By inscribing the rocking LPG on this fiber,

two polarization-dependant resonant dips will be shifted due to the change of external environment. The responses of the wavelength dips (the fast and slow mode resonance dips) to high temperature and refractive index can be different due to the coupling with different cladding modes, so simultaneous measurement of high temperature and refractive index can be achieved through [16]

$$\Delta\lambda_F = A\Delta T + B\Delta R, \Delta\lambda_S = C\Delta T + D\Delta R, \quad (7)$$

$$\begin{bmatrix} \Delta T \\ \Delta R \end{bmatrix} = \begin{bmatrix} A & B \\ C & D \end{bmatrix} \begin{bmatrix} \Delta\lambda_F \\ \Delta\lambda_S \end{bmatrix}, \quad (8)$$

where  $\Delta\lambda_F$  and  $\Delta\lambda_S$  are respectively the wavelength shifts of fast mode and slow mode resonance dips, induced by high temperature variation  $\Delta T$  and gas pressure  $\Delta R$ ,  $A$  and  $B$  are high temperature coefficient and refractive index coefficient of fast mode resonance dip, and those corresponding to slow mode resonance dip are  $C$  and  $D$ . The equation will be

$$\begin{bmatrix} \Delta T \\ \Delta R \end{bmatrix} = \begin{bmatrix} -10.51 & 0.106 \\ -2.4 & 0.085 \end{bmatrix} \begin{bmatrix} \Delta\lambda_F \\ \Delta\lambda_S \end{bmatrix}. \quad (9)$$

The refractive index responses of the PR-LPG are tested by immersing the device into refractive index oil. The refractive index sensitivity is obtained by monitoring the resonant wavelength shift from 1.3 to 1.4 with the step of 0.02. The two resonant wavelengths corresponding to the two polarization states as a function of refractive index are shown in Fig.8.

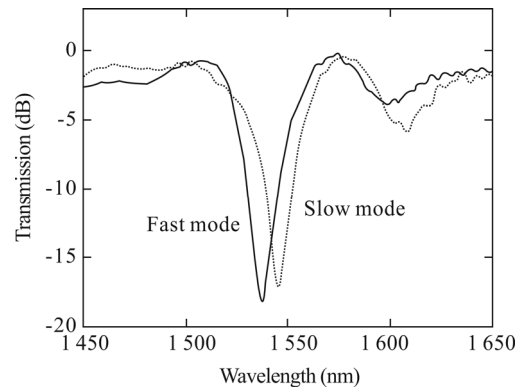


**Fig.5 Spectra of a rocking LPG fabricated in PANDA fiber with 3.5° twist angle and 8 periods**

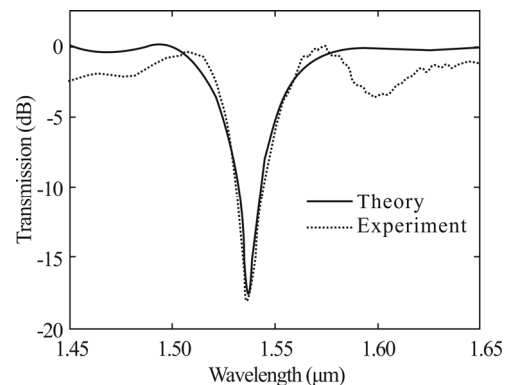


**Fig.6 Comparison of calculated and measured transmission spectra of a PR-LPG**

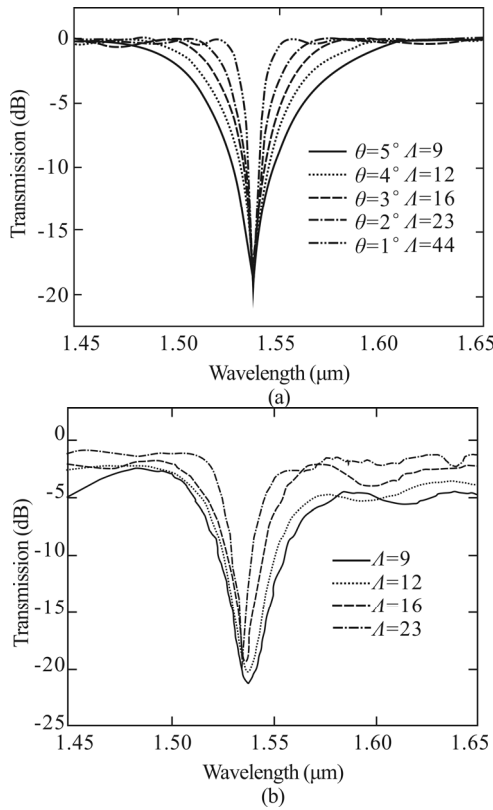


**Fig.7 (a) Calculated and (b) measured transmission spectra of PR-LPGs with different twist angles**

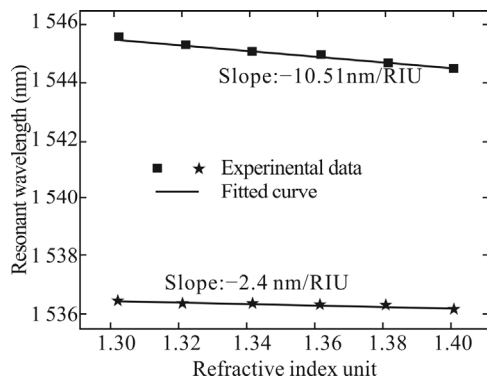


**Fig.8 Resonant wavelength as a function of refractive index**

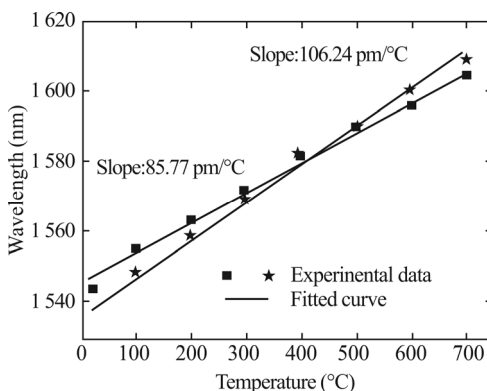


**Fig.9 Resonant wavelength as a function of high temperature**

The high temperature responses of the PR-LPG are tested with a high temperature furnace. Before tests, the grating was heated from 22 °C to 700 °C at an average rate of 10 °C/min and pre-annealed at 700 °C for 1 h. Then the high temperature sensitivity is obtained by monitoring the resonant wavelength shift from 22 °C to 700 °C with the step of 100 °C. The shifts of resonant wavelengths with high temperature are shown in Fig.9.

A PR-LPG is fabricated in a PANDA fiber by scanning a CO<sub>2</sub> laser beam transversely across the fiber while it is twisted alternatively. Theoretical and experimental results demonstrate that the twist angle can affect the resonance coupling. Very efficient polarization-selective resonant coupling is achieved for a grating with 13 periods and just one scanning cycle. The responses of such a rocking LPG fabricated in PANDA fiber to high temperature and refractive index are experimentally investigated. The two polarization-selective resonance dips show different coefficients, which can be used for simultaneous measurements.

**References**

- [1] A. M. Vengsarkar, J. R. Pedrazzani, J. B. Judkins, P. J. Lemaire, N. S. Bergano and C. R. Davidson, *Opt. Lett.* **21**, 336 (1996).
- [2] V. Bhatia and A. M. Vengsarkar, *Opt. Lett.* **21**, 692 (1996).
- [3] Ji L, Liu T, He G, Sun X, Wang X, Yi Y, Chen C, Wang F and Zhang D, *IEEE Photonics Technology Letters* **28**, 633 (2016).
- [4] Ahmed F, Joe H E, Min B K and Jun M B G, *Optics & Laser Technology* **74**, 119 (2015).
- [5] Dong J and Chiang K S, *IEEE Photonics Technology Letters* **27**, 1006 (2015).
- [6] Yong Y T, *Journal of Electromagnetic Waves & Applications* **29**, 703 (2015).
- [7] Wang L, Zhang W, Chen L, Bai Z, Liu F and Yan T, *Journal of Modern Optics* **5**, 1 (2017).
- [8] Chu J, Shen C, Qian F, Zhong C, Zou X, Dong X, Jin Y, Wang J, Gong Y and Jiang T, *Optical Fiber Technology* **20**, 44 (2014).
- [9] Qingquan Wang, Yunqi Liu, Liang Zhang and Tingyun Wang, *Appl. Opt.* **56**, 4325 (2017).
- [10] T. Zhu, Y. J. Rao and J. L. Wang, *Appl. Opt.* **46**, 375 (2007).
- [11] Ivanov O V, *Opt. Lett.* **30**, 3290 (2005).
- [12] N D. Tian, Y. Liu, X. Cao, L. Zhang and T. Wang, *Sensing Characteristics of CO<sub>2</sub>-laser Written Helical Long-period Fiber Gratings*, *Optical Communications and Networks*, 1 (2016).
- [13] G. Statkiewicz-Barabach, A. Anuszkiewicz, W. Urbanczyk and J. Wojcik, *Opt. Exp.* **16**, 17258 (2008).
- [14] R. Ulrich and A. Simon, *Appl. Opt.* **18**, 2241 (1979).
- [15] Yiping Wang, D. N. Wang, Wei Jin, Hoi Lut Ho and Jian Ju, *Opt. Commun.* **281**, 2522 (2008).
- [16] M. Sudo, M. Nakai, K. Himeno, S. Suzuki, A. Wada and R. Yamauchi, *Simultaneous Measurement of Temperature and Strain using PANDA Fiber Grating*, 12th International Conference on Optical Fiber Sensors, 1997.